Theoretical Study of the Cosolvent Effect on the Partial Molar Volume Change of Staphylococcal Nuclease Associated with Pressure Denaturation

Takeshi Yamazaki

Department of Mechanical Engineering, University of Alberta, and National Institute for Nanotechnology, National Research Council of Canada, 11421 Saskatchewan Drive, Edmonton, Alberta T6G 2M9, Canada

Takashi Imai

Department of Bioscience and Bioinformatics, Ritsumeikan University, Kusatsu, Shiga 525-8577, Japan

Fumio Hirata

Department of Theoretical Studies, Institute for Molecular Science, Okazaki, Aichi 444-8585, Japan

Andriy Kovalenko*

National Institute for Nanotechnology, National Research Council of Canada, and Department of Mechanical Engineering, University of Alberta, 11421 Saskatchewan Drive, Edmonton, Alberta T6G 2M9, Canada

Received: July 20, 2006; In Final Form: October 30, 2006

We explain the molecular mechanism of the effect of urea and glycerol cosolvents on the partial molar volume (PMV) change associated with the pressure denaturation of staphylococcal nuclease (SNase) protein recently observed in experiments. Native and denatured conformations of SNase are produced by using molecular dynamics simulations in water, and the PMV is obtained from the integral equation theory of molecular liquids called 3D-RISM, which is based on statistical mechanics. The PMV of the native SNase in water predicted by 3D-RISM theory is in good agreement with experiment. The PMV changes associated with pressure denaturation in water and in water−urea and water−glycerol mixtures are qualitatively reproduced. By analyzing the results obtained, we found two interesting cosolvent effects on the PMV: (1) both urea and glycerol cosolvents increase the PMVs of both native and denatured SNase compared to those in water and (2) both urea and glycerol cosolvents increase the PMV of denatured SNase more than that of native SNase. We also showed that these two observations can be explained in terms of the thermal volume, which is related to the packing effect of solvent molecules.

1. Introduction

The partial molar volume (PMV) of protein has drawn much attention as one of the most fundamental thermodynamic quantities used to characterize the conformational stability of proteins,[1] especially in the analysis of pressure-induced denaturation of proteins from the viewpoint of Le Chatelier's law.[2] When pressure is applied, the thermodynamic stability of native a protein is modulated, and as a result, the protein changes its structure to one with a smaller PMV value.[3] Recently, Akasaka and co-workers[4−6] proposed the "volume theorem" of protein folding on the basis of a high-pressure NMR measurement. They claim that the PMV of a protein generally decreases in parallel with the loss of its conformational order. In other words, PMV could be an order parameter in protein folding and conformational changes, which would enable us to advance the understanding of mechanisms of protein functioning.

The thermodynamic stability of a protein can be modulated not only by thermodynamic variables, such as pressure, but also by solvent conditions. The native protein is known to be marginally stable along temperature and pressure axes as well as under the chemical conditions of the solvent.[7] Several studies have investigated the change in the protein volume associated with pressure denaturation in the presence of cosolvents.[8−14] Recently, Winter and co-workers[15] studied the effects of various chaotropic and kosmotropic cosolvents (glycerol, sucrose, sorbitol, K_2SO_4, $CaCl_2$, and urea) on the secondary structure and thermodynamic properties upon unfolding and denaturation of staphylococcal nuclease (SNase) by using FTIR spectroscopy. SNase has been widely employed as a model for understanding protein folding because it is a small (149 amino acid), single-domain, monomeric protein that contains no sulfhydryl residues or disulfide linkages. The data show that different cosolvents have a profound effect on the denaturation pressure and the changes in the Gibbs free energy and PMV with unfolding.

In the present article, we study the cosolvent effect on the PMV change associated with pressure denaturation of SNase, choosing urea and glycerol as cosolvents. According to the experiment by Winter and co-workers,[15] the volume change of denaturation has been determined to be -66 ± 8 cm^3/mol for the pure SNase buffer solution, whereas volume changes of about -55 and -60 cm^3/mol have been determined for the 0.5 M concentration of glycerol and urea, respectively. That is, a slight decrease (about $5-10$ cm^3/mol) in the absolute value of volume changes has been observed for the concentration of

* Corresponding author. E-mail: andriy.kovalenko@nrc-cnrc.gc.ca.

10.1021/jp064615f CCC: $37.00
Published on Web 01/11/2007

glycerol and urea compared to that of pure buffer solution. How and why do both the urea and the glycerol cosolvents decrease the PMV changes? This is not a trivial question at all, and this is our concern in the present study.

Since Kitchen et al.[16] investigated bovine pancreatic trypsin inhibitor under high pressure by molecular dynamics (MD) simulation, almost all theoretical studies of proteins under high pressure used molecular simulations and provided useful information about the response of native proteins to external pressure.[17] However, when it comes to the PMV of a protein in solution, reliable estimates from molecular simulation are hopeless. The PMV is a derivative of the solvation free energy, and the evaluation of the latter is already one of the most difficult tasks for the method. Fortunately, the statistical mechanical theory of liquids provides the way to determine the PMV of proteins quantitatively. Therefore, to answer the questions of how and why the urea and glycerol cosolvents decrease the PMV changes, we use both MD simulations and the integral equation theory of molecular liquids, which is based on statistical mechanics. The latter is called the 3D reference interaction site model (3D-RISM) theory.[18−22] MD simulations are used to obtain the conformations of proteins, and the 3D-RISM theory is applied to obtain the PMV of proteins having various (fluctuating) conformations generated by the MD simulation. It has been reported that the PMV calculated by the 3D-RISM theory is in quantitative agreement with experimental data.[23] This kind of combination, molecular simulation plus integral equation theory, would be one of the most promising ways to study the thermodynamics of macromolecules in solution. Although there has been a suggestion that the experimentally observed changes of PMV in the presence of cosolvents are affected by protein−protein interaction,[24] we first study the protein solvated in aqueous solutions at infinite dilution in order to isolate, elucidate, and explain the cosolvent effect on PMV change observed in the experiment.[15]

2. Methods

2.1. All-Atom Molecular Dynamics Simulations. To construct the SNase protein, the crystallographic structure of SNase was taken from the PDB structure 1STN. This lacks residues 1−5 and 142−149, which were disordered in the crystal. The starting structure for the MD simulation was completed by adding coordinates for residues 1−5 (taken from the PDB structure 2SNS) and constructing residues 142−149. Much as in the previous MD simulation for SNase,[25] all histidines were assumed to be uncharged. His8, His121, and His124 were assumed to be protonated at the δ site, and His46 was assumed to be protonated at the ϵ site. The SNase protein was then solvated using the Solvate plug-in of VMD[26] to create a periodic water cell of size ∼(80 × 94 × 86) Å^3 accommodating the solvation shell of about 20 Å around the protein. The system contained 19 647 water molecules (including 83 crystallographic water molecules in 1STN), and 8 chloride ions were added to neutralize the system. The entire system was then minimized to remove unfavorable contacts and reduce the strain in the system.

The MD simulations were performed in the CHARMM22 force field[27] with the TIP3P water model[28] by using the MD program NAMD2.[29] Constant temperature was maintained using weakly coupled Langevin dynamics of nonhydrogen atoms; pressure was maintained using the Langevin piston Nose-Hoover barostat with an oscillation period of 200 fs and a decay time of 100 fs. All hydrogen bonds were constrained during the simulations using the SHAKE algorithm, and an integration time

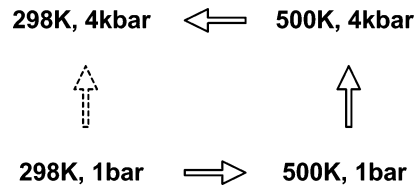

Figure 1. Thermodynamic cycle used to obtain pressure-induced denatured SNase.

step of 1 fs was used. Full electrostatic forces were evaluated using the particle-mesh Ewald method with an 80 × 96 × 88 point grid. Short-range nonbonded terms were evaluated at every step using a 12 Å cutoff for the van der Waals interactions and a smooth switching function. We ran the simulations along the pathways shown in the schematic thermodynamic cycle (Figure 1). In the simulation at elevated pressure, a gradient of 1 kbar/500 ps was used until a pressure of 4 kbar was attained. The overall simulation time was ∼15 ns.

2.2. 3D-RISM Theory and Partial Molar Volume. To calculate the PMVs, we obtain the 3D correlation functions between SNase and solvent molecules from the 3D-RISM theory[18−22] and calculate PMVs through the Kirkwood−Buff (KB) theory[30] coupled with the 3D-RISM method (3D-RISM-KB).[31] The details of the RISM theory have been given in the literature, and here we provide a brief outline.

The 3D-RISM equation[18−21]

$$h_\gamma(\mathbf{r}) = \sum_{\gamma'} \int \mathrm{d}\mathbf{r}'\, c_{\gamma'}(\mathbf{r}')\, \chi_{\gamma'\gamma}(|\mathbf{r} - \mathbf{r}'|) \tag{1}$$

is coupled with the 3D version of the closure approximation proposed by Kovalenko and Hirata (3D-KH closure)[18,21]

$$g_\gamma(\mathbf{r}) = \begin{cases} \exp(\mathrm{d}_\gamma(\mathbf{r})) - 1 & \text{for } \mathrm{d}_\gamma(\mathbf{r}) \le 0 \\ \mathrm{d}_\gamma(\mathbf{r}) & \text{for } \mathrm{d}_\gamma(\mathbf{r}) > 0 \end{cases} \tag{2a}$$

$$\mathrm{d}_\gamma(\mathbf{r}) = -\frac{u_\gamma(\mathbf{r})}{k_\mathrm{B}T} + h_\gamma(\mathbf{r}) - c_\gamma(\mathbf{r}) \tag{2b}$$

Here, $h_\gamma(\mathbf{r})$ is the 3D total correlation function, which is related to the 3D distribution function $g_\gamma(\mathbf{r}) = h_\gamma(\mathbf{r}) + 1$ giving the normalized probability of finding the interaction site γ of solvent molecules at position $\mathbf{r}$ around the solute molecule. $c_\gamma(\mathbf{r})$ is the 3D direct correlation function, which has the asymptotics of the solute−solvent site interaction potential: $c_\gamma(\mathbf{r}) \approx -u_\gamma(\mathbf{r})/(k_\mathrm{B}T)$, where $k_\mathrm{B}T$ is the Boltzmann constant times the temperature. The solvent susceptibility $X_{\gamma'\gamma}(r) = \omega_{\gamma'\gamma}(r) + \rho_{\gamma'} h_{\gamma'\gamma}(r)$ splits up into the intramolecular distribution function $\omega_{\gamma'\gamma}(r)$, specifying the geometry of solvent molecules, and the intermolecular site−site total correlation function $h_{\gamma'\gamma}(r)$ times the solvent-site number density $\rho_{\gamma'}$. The radial correlations of pure solvent are obtained, in advance of the 3D-RISM-KH calculation, from the RISM integral equation theory coupled with the KH closure (RISM-KH).[18,22] The convolution in eq 1 is calculated by using the 3D fast Fourier transform technique, with special analytical treatment of the electrostatic asymptotics of all of the correlation functions (both 3D and radial ones).[18,22]

The partial molar volume $\bar{V}$ is obtained from the 3D direct correlation functions $c_\gamma(\mathbf{r})$ on the basis of the 3D-RISM-KB theory[31]

$$\bar{V} = k_\mathrm{B}T\chi_\mathrm{T}\left(1 - \rho \sum_\gamma \int_{V_\mathrm{cell}} \mathrm{d}\mathbf{r}\, c_\gamma(\mathbf{r})\right) \tag{3}$$

where χ_T is the isothermal compressibility of pure solvent, which

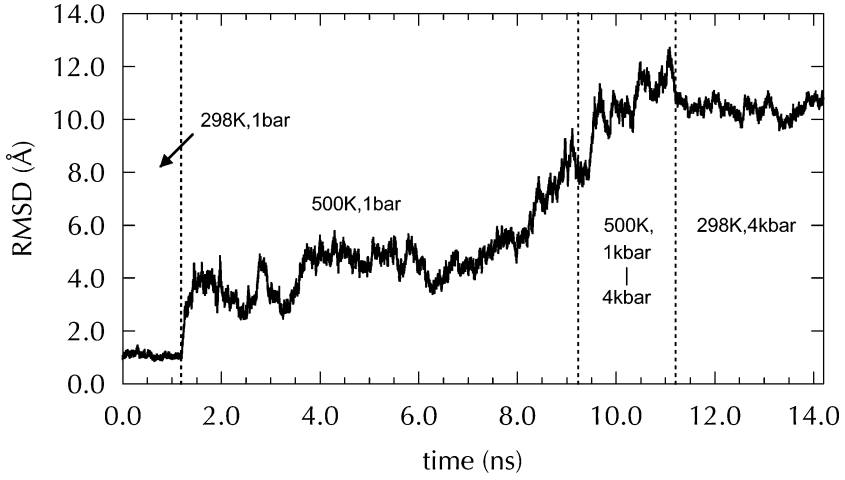

Figure 2. Root-mean-square deviation of the backbone heavy atoms of SNase from the crystallographic structure.

can be obtained from the RISM-KH theory for the solvent−solvent correlation functions.

We considered water and 0.5 M water−urea and water−glycerol mixtures with densities of 0.9980, 1.005, and 1.009 g/cm^3, respectively, corresponding to the ambient conditions of $T = 298.15$ K and a pressure of 1 bar. The 3D-RISM-KH eqs 1 and 2 were solved on a grid of 128 × 128 × 128 points in a cubic supercell of size 128 × 128 × 128 Å^3, which is sufficiently large to accommodate the protein molecule with sufficient solvation space around it. The convergence threshold was determined for the convergence error in the PMV to be less than 1 cm^3/mol.

We used the CHARMM22 force field for the protein and the TIP3P model for water, much as in the present MD simulation. We employed the OPLS force field parameters for the urea[32] and glycerol[33] molecules. Concerning the geometries of the urea and glycerol molecules, we used the planar conformation of urea[32] and the stable conformation of glycerol determined theoretically.[34]

3. Results and Discussion

3.1. Native and Denatured Protein Conformations by MD Simulation. To obtain the native and denatured SNase conformations, we ran MD simulations along the pathway shown by open arrows in Figure 1. The denaturation pathway along the pressure axis on the $T-P$ phase diagram of the protein (dotted arrow in Figure 1) is a prohibitively time-consuming task for the molecular simulations[17,35−37] because the application of high pressure slows down the protein conformation dynamics in MD simulations. To circumvent this problem, we used the following pathway for the denaturation conformations under high pressure in the present study. First, we ran a 1 ns simulation for the native protein at room temperature (298.15 K) and 1 bar of pressure. Next, we carried out a long-time simulation under a high temperature of 500 K at 1 bar of pressure to denature the protein briefly. We then increased the pressure of the system up to 4 kbar at $T = 500$ K and finally decreased the system temperature to room temperature under the same pressure of 4 kbar. Other treatments used to circumvent this difficulty are worth mentioning. Paliwal et al.[36] have combined random insertions of water into the protein interior with MD simulations at progressively higher pressure to produce the onset of pressure unfolding. García and co-workers[38,39] have applied an extension of the replica-exchange MD method for temperature- and pressure-induced unfolding of peptides.

Figure 2 gives the root-mean-square (rms) deviation of the backbone heavy atoms of SNase from the crystallographic structure as a function of time. After 200 ps of equilibration, the system appeared to be well equilibrated, and we started the 1 ns simulation at $T = 298.15$ K under 1 bar. We then carried out 8 ns runs at 500 K under 1 bar. The rms deviation between the MD structures and the crystallographic structure gradually became large, and the protein began to denature after about 8 ns. As the pressure was elevated from 1 bar to 4 kbar at 500 K, the rms deviation became larger and the denaturation progressed further. We then cooled the system temperature down to 298.15 K under 4 kbar and equilibrated the system. To calculate PMVs by using the 3D-RISM theory, we picked out 100 conformations from the 1 ns trajectory (a conformation every 10 ps) for the native SNase after 200 ps of equilibration and picked out another set of 100 conformations from the last 1 ns trajectory for the denatured SNase. The snapshots of the 100th native and denatured conformations are shown in Figure 3. In the native state, SNase has a hydrophobic core shown by the gray circle in Figure 3a. As the simulation progresses, water molecules gradually penetrate the inside of the core, and as a result of penetration, this protein forms two subdomains separated as shown in Figure 3b. This denatured conformation is in qualitative agreement with the recent experiment using small-angle neutron scattering by Paliwal et al.[36] Their results have suggested that the denatured SNase under high pressure forms two separate subdomains.

3.2. Three-Dimensional Solvation Structure around Protein. In Figures 4 and 5, we present the isosurface representations of the 3D solvation structure by the 3D distribution functions $g_\gamma(\mathbf{r})$ of solvent site γ around the native and denatured SNase, obtained from the 3D-RISM theory. The SNase conformations in Figures 4 and 5 are the same as in Figure 3. To visualize the 3D solvation structures, we focus our attention on the atomic sites closest to the center of solvent molecules: the oxygen site of water, the carbon site of urea, and the C2 carbon of glycerol molecules. We depict the isosurfaces of $g(\mathbf{r}) > 2$, that is, the areas where the probability density of finding a solvent molecule is twice as large as in the solvent bulk. In the space-filling model of the protein, the hydrophobic residues are indicated in gray, and the polar ones are indicated in white. Figure 4a−c shows the $g(\mathbf{r})$ of water oxygen (blue) around native protein solvated in water and water−urea and water−glycerol mixtures, respectively. Figure 4d,e shows the $g(\mathbf{r})$ of urea carbon (red) and of glycerol C2 carbon (green). In a similar

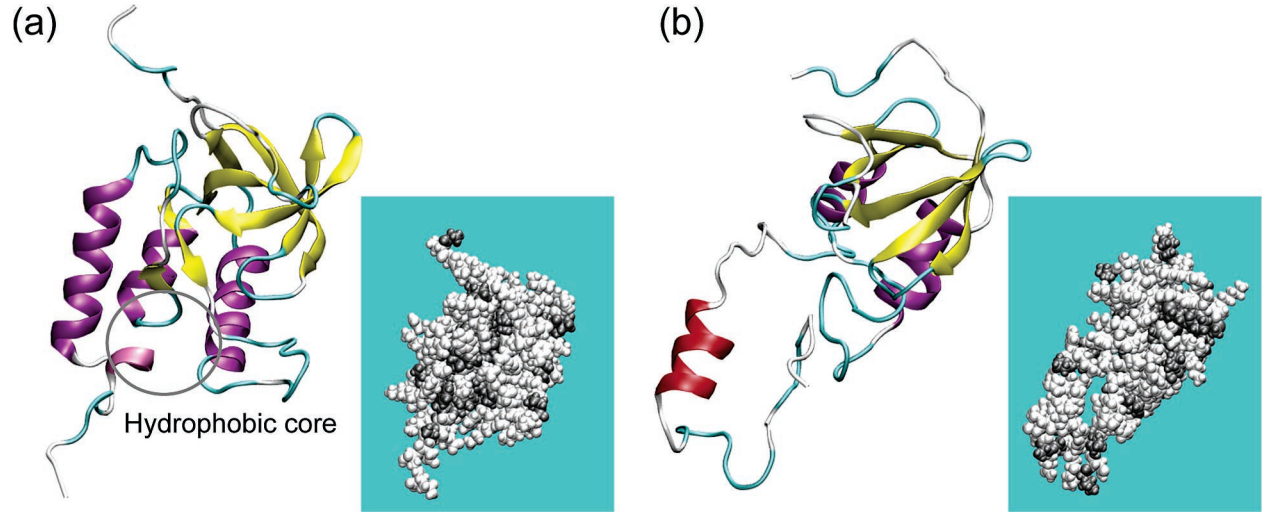

Figure 3. Native SNase (a) and resulting denatured SNase under high pressure (b). The gray circle in part (a) shows the hydrophobic core. A cartoon representation is shown together with the space-filling model. In the space-filling model, the hydrophobic and polar residues are shown in gray and white, respectively.

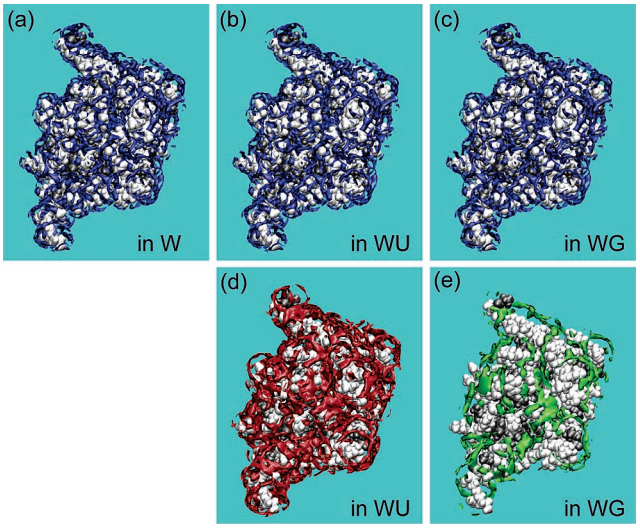

Figure 4. Isosurface representation of the 3D distribution function of water oxygen (blue), urea carbon (red), and glycerol C2 carbon (green) around native SNase. The surfaces show the areas of the distribution function $g(\mathbf{r}) > 2$. The SNase protein is represented by the space-filling model with the hydrophobic and polar residues shown in gray and white, respectively.

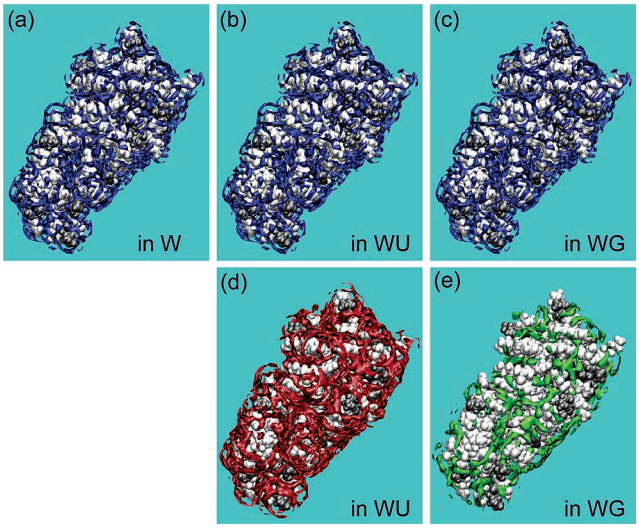

Figure 5. Same as in Figure 4 but for denatured SNase.

way, we present $g(\mathbf{r})$ for the denatured protein. According to the above Figures, water molecules are distributed mainly around polar residues and are not strongly perturbed by the cosolvent at the low concentration we consider here. The cosolvents are also distributed mainly around the polar residues. By comparing the areas of $g(\mathbf{r})$ in the Figures, we can see that glycerol molecules are less spread over the protein surface than are water molecules. The oxygen sites of glycerol (data not shown), which form hydrogen bonds with the protein, much as water oxygens do, are also spread less than the water oxygens. This might be an indication of the exclusion of glycerol or preferential hydration of the protein.[40−43]

3.3. PMV Change Associated with Denaturation. In Figure 6, the values of PMV for each native-state conformation of SNase in water predicted by the 3D-RISM theory are plotted along with the experimental value obtained by Filfil and Chalikian.[44] As we can see from this Figure, the theory reproduces the experimental value of PMV well. The PMV values of for almost all of the conformations are within the

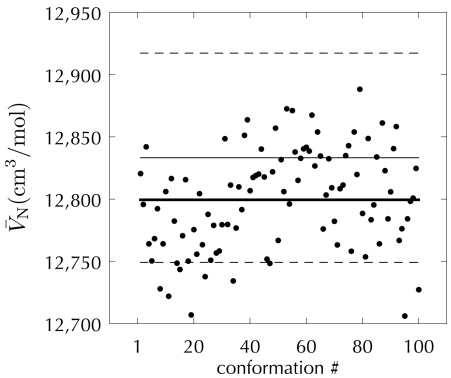

Figure 6. Partial molar volume of native SNase in water. The calculated values of PMV for each native conformation (●) and their average (—). The experimental data[44] (−) and its confidence interval (--).

confidence interval of the experimental data. In a similar way, we calculated the PMVs of denatured SNase protein in water and in water−urea and water−glycerol mixtures. Table 1 compiles the predictions of 3D-RISM for the PMVs in the native and denatured states, $\bar{V}_N$ and $\bar{V}_D$, averaged over the conformations, and it compiles the corresponding PMV change $\bar{V}_D - \bar{V}_N$ associated with denaturation. In every case, we obtained a

TABLE 1. PMV (cm^3/mol) of the Native and Denatured States, $\bar{V}_N$ and $\bar{V}_D$, and the PMV Change $\bar{V}_D - \bar{V}_N$ Associated with Denaturation in Water and in Water−Urea and Water−Glycerol Mixtures[a]

	in water	in water−urea	in water−glycerol
$\bar{V}_N$	12 800	12 810	12 816
$\bar{V}_D$	12 619	12 632	12 640
PMV change	−181	−178	−176

[a] Predictions of the 3D-RISM theory.

negative PMV change associated with denaturation, as observed in the experiments for pressure-induced denaturation. Given that the range of the PMV change for SNase has been reported to be between −27 and −112 cm^3/mol,[3] our theoretical predictions fall in a considerably reasonable range. Furthermore, although the difference is very small, both the urea and glycerol cosolvents decrease the PMV change compared to that in water. This is in agreement with the experimental results of Winter and co-workers[15] discussed in the Introduction.

3.4. Cosolvent Effect on the PMV Change. Now we are able to answer the question of how and why both the urea and the glycerol cosolvents decrease the PMV change associated with denaturation compared to that in pure water. Figure 7 shows the cosolvent effects on the PMV of native and denatured SNase, $\Delta\bar{V}_N(W \rightarrow Mix)$ and $\Delta\bar{V}_D(W \rightarrow Mix)$. For example, the cosolvent effect of urea on PMV of the native SNase means the difference between the PMV of native SNase in water (W) and that in a water−urea mixture (WU), that is, $\Delta\bar{V}_N(W \rightarrow WU) = \bar{V}_N(\text{in WU}) - \bar{V}_N(\text{in W})$. Two interesting observations for the effect of the urea and glycerol cosolvents on the PMVs follow from Figure 7:

(1) The cosolvents increase the PMVs of both native and denatured SNase compared to those in water.

(2) The cosolvents increase the PMV of denatured SNase more than that of native SNase.

To analyze the origin of these changes further, we decomposed the cosolvent effect on the PMV into nonelectrostatic and electrostatic contributions: $\Delta\bar{V}(W \rightarrow Mix) = \Delta\bar{V}^{non-e}(W \rightarrow Mix) + \Delta\bar{V}^{elec}(W \rightarrow Mix)$. The nonelectrostatic part of the PMV of native and denatured conformations, $\Delta\bar{V}_N^{non-e}(W \rightarrow Mix)$ and $\Delta\bar{V}_D^{non-e}(W \rightarrow Mix)$, respectively, was obtained by applying 3D-RISM to the solvated protein with all of its partial site charges switched off (with only van der Waals interactions between SNase and solvents taken into account). The rest of the PMV change for the protein with full charges, $\Delta\bar{V}_N(W \rightarrow Mix)$ and $\Delta\bar{V}_D(W \rightarrow Mix)$, was attributed to the electrostatic part $\Delta\bar{V}_N^{elec}(W \rightarrow Mix)$ and $\Delta\bar{V}_D^{elec}(W \rightarrow Mix)$. Figure 8 shows the results of this decomposition. $\Delta\bar{V}^{elec}$ is negative in each case, which suggests that the so-called electrostriction effect is larger in the mixture than in water. However, $\Delta\bar{V}^{non-e}$ is positive and larger in magnitude than $\Delta\bar{V}^{elec}$. Moreover, $\Delta\bar{V}^{non-e}$ in the denatured state is larger than that in the native state. This decomposition clearly tells us that the nonelectrostatic part of PMV dominates in the cosolvent effect on the PMV change associated with denaturation, resulting in the above observations (1 and 2).

3.5. Molecular Mechanism of the Cosolvent Effect on the PMV Change. It is well known that in aqueous solution the PMV of a nonpolar (chargeless) solute is larger than its van der Waals volume. Chalikian and Breslauer[45] have introduced "thermal volume" to fill the difference between them. Thermal volume is a contribution from thermally induced, molecular vibrations of both the solute and the solvent molecules that leads to additional expansion of the solvent accommodating the solute

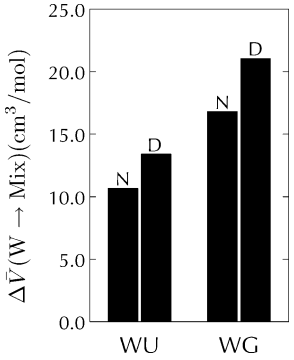

Figure 7. Cosolvent effect of urea (left) and glycerol (right) on the partial molar volume of native (N) and denatured (D) protein.

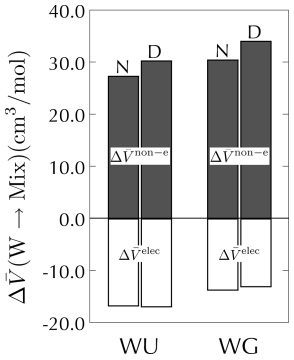

Figure 8. Decomposition of the cosolvent effect on the partial molar volume into electrostatic (white) and nonelectrostatic (gray) parts.

molecule. This expansion has been viewed as creating an empty space around the solute molecule.[46,47] Intuitively, this is related to how solvent molecules are packed around the solute molecule, which is called the packing effect. For example, if solvent molecules are well packed around the solute molecule and the empty space is negligible, then the thermal volume is also negligible, and the solute PMV is almost the same as its van der Waals volume.

In the above decomposition (Figure 8), we obtained $\Delta\bar{V}^{non-e}$ as the difference between the nonelectrostatic contribution $\bar{V}^{non-e}$ for chargeless SNase in the mixture of solvents and that for water. The nonelectrostatic part $\bar{V}^{non-e}$ further consists of four contributions: an ideal term, the van der Waals volume, the void volume, and the thermal volume.[48,49] The ideal term is the volume related to the kinetic contribution to the pressure of an ideal gas at temperature T due to translational degrees of freedom and is given by $k_BT\chi_T$, where χ_T is the isothermal compressibility of the solvent. It was found that the change in the ideal term of PMV from water to the solvent mixture is negligible (the ideal term was calculated to be 1.21 cm^3/mol in water, 1.21 cm^3/mol in water−urea, and 1.22 cm^3/mol in the water−glycerol mixture.) The van der Waals volume and the void volume, that is, the volume of structural voids within the solvent-inaccessible core of the protein molecule, provide the molecular volume of the protein itself. Because we have used the same protein conformations for every solvent, we have the same molecular volume of SNase in these solutions. Therefore, the nonelectrostatic part $\Delta\bar{V}^{non-e}$ comes only from the difference between the thermal volume (packing effect) in the solvent mixture and that in water.

The molecular volumes of both the urea and the glycerol molecules are larger than that of the water molecule. Regarding solvent molecules for simplicity as spherical particles, we immediately see that the empty space between the protein surface and a layer of cosolvent molecules is larger than that

between the protein and water molecules. This increases the thermal volume in the solvent mixture to a value larger than that of water and makes $\Delta\bar{V}^{\mathrm{non-e}}$ positive for both native and denatured proteins. Furthermore, the protein denatured under high pressure allows the solvent molecules to access not only its surface but also the inside of the protein core and exposes the hydrophobic residues that are hidden in the native state. These processes contribute to making the solvent-accessible surface area (SASA) of the protein larger. By using VMD[26] with a probe radius of 1.4 Å, we calculated the average values of SASA for the 100 native and 100 denatured proteins to be 9951 and 11 462 Å^2, respectively. As we have seen in Figures 4 and 5, not only water but also urea and glycerol cosolvents have access to the protein surface and are actually spread over it in both the native and the denatured states. Thus, we expect the empty space between the denatured protein and solvents to be larger than that for the protein in the native state. Therefore, the molecules of cosolvent larger than water increase the PMV of denatured SNase more than that of native SNase, in proportion to the SASA difference. This argument on the packing effect explains our decomposition results and the PMV changes observed in the experiment.[15]

It should be noted here that a protein can change its conformation in such a way that the protein surface fits not only the water but also the cosolvent molecules, especially at high concentrations of cosolvent. In the present study, we investigated the PMVs of protein solvated in water and water−cosolvent mixtures using the protein conformations obtained by MD simulations in water and assuming that the cosolvent concentration of 0.5 M is dilute enough so as not to cause a large change in the protein conformation compared to that in water. In the case of a cosolvent at higher concentration, however, the protein conformation may adjust for the molecular volume (shape) of the cosolvent, resulting in another scenario for the cosolvent effect on the PMV change associated with pressure denaturation.

4. Conclusions

One of the most fundamental thermodynamic quantities characterizing the conformational stability of a protein in solution under pressure is the partial molar volume (PMV). According to the recent suggestions from experiments by Akasaka and co-workers,[4−6] the PMV might be considered to be an order parameter in protein folding and conformational changes, which has substantial implications on the understanding of protein functions. By employing the novel statistical-mechanical approach of the molecular theory of solvation called 3D-RISM, we have been uniquely able to predict and elucidate the cosolvent effect on the PMV of protein. This is not feasible by using just molecular simulations.

In this article, we have explained how and why the urea and glycerol cosolvents affect the PMV change associated with pressure-induced denaturation of the SNase protein. Native and denatured conformations of SNase have been prepared by using the MD simulation in water, whereas the PMVs in water and in water−urea and water−glycerol mixtures have been obtained by using the 3D-RISM theory. The PMV of the native SNase in water predicted by the theory is in good agreement with the experiment, and the PMV changes associated with pressure denaturation in water and in water−urea and water−glycerol mixtures are qualitatively reproduced. By analyzing the results obtained, we have found the following: (1) the cosolvents increase the PMVs of both native and denatured SNase compared to those in water and (2) the cosolvents increase the PMV of denatured SNase more than that of native SNase. These two observations can be explained by the solvent packing effect as follows. Because the molecular volumes of the cosolvents are larger than that of the water molecule, the empty space between the protein surface and cosolvent molecules is larger than that between the protein and water molecules. This increases the PMV in a mixture more than in water. Furthermore, the denaturation under high pressure allows solvent molecules to access the inside of the protein, also exposing the hydrophobic residues otherwise hidden in the native state. Therefore, the solvent-accessible surface area and hence the empty spaces between the solvents and the protein get larger in the denatured state than in the native one. Accordingly, the larger cosolvent molecules creating larger empty spaces increase the PMV of denatured SNase more than that of native SNase. As a result, the PMV change associated with pressure denaturation decreases upon addition of cosolvents. This constitutes the molecular mechanism of the effect of the urea and glycerol cosolvents at low concentration on the PMV change in pressure-induced denaturation, which is observed in the experiment.

Acknowledgment. We gratefully acknowledge the financial support of the National Research Council of Canada (T.Y. and A.K.) and of the Japanese Ministry of Education, Culture, Sports, Science, and Technology (T.I. and F.H.). A.K. and T.Y. are also grateful to the National Science and Engineering Research Council of Canada for the financial support from NSERC Individual Discovery Grant No. 314090-05. T.Y. is thankful to Professor Yoshihiro Taniguchi of Ritsumeikan University and Professor Kazuyuki Akasaka of Kinki University for their helpful comments and fruitful discussions. This research has been enabled by the use of WestGrid computing resources, which are funded in part by the Canada Foundation for Innovation, Alberta Innovation and Science, BC Advanced Education, and the participating research institutions. WestGrid equipment is provided by IBM, Hewlett-Packard and SGI. Figures 3−5 were produced with the visualization program VMD.[26]

References and Notes

(1) Chalikian, T. V. *Annu. Rev. Biophys. Biomol. Struct.* **2003**, *32*, 207.
(2) Balny, C.; Masson, P.; Heremans, K. *Biochim. Biophys. Acta* **2002**, *1595*, 3.
(3) Royer, C. A. *Biochim. Biophys. Acta* **2002**, *1595*, 201.
(4) Kitahara, R.; Yamada, H.; Akasaka, K.; Wright, P. E. *J. Mol. Biol.* **2002**, *320*, 311.
(5) Kitahara, R.; Akasaka, K. *Proc. Natl. Acad. Sci. U.S.A.* **2003**, *100*, 3167.
(6) Akasaka, K. *Biochemistry* **2003**, *42*, 10 875.
(7) Scharnagl, C.; Reif, M.; Friedrich, J. *Biochim. Biophys. Acta* **2005**, *1749*, 187.
(8) Pappenberger, G.; Saudan, C.; Becker, M.; Merbach, A. E.; Kiefhaber, T. *Proc. Natl. Acad. Sci. U.S.A.* **2000**, *97*, 17.
(9) Ruan, K.; Xu, C.; Yu, Y.; Li, J.; Lange, R.; Bec, N.; Balny, C. *Eur. J. Biochem.* **2001**, *268*, 2742.
(10) Webb, J. N.; Webb, S. D.; Cleland, J. L.; Carpenter, J. F.; Randolph, T. W. *Proc. Natl. Acad. Sci. U.S.A.* **2001**, *98*, 7259.
(11) Perrett, S.; Zhou, J. M. *Biochim. Biophys. Acta* **2002**, *1595*, 210.
(12) Skerjanc, J.; Dolecek, V.; Lapanje, S. *Eur. J. Biochem.* **1970**, *17*, 160.
(13) Skerjanc, J.; Lapanje, S. *Eur. J. Biochem.* **1972**, *25*, 49.
(14) Lee, J. C.; Timasheff, S. N. *Biochemistry* **1974**, *13*, 257.
(15) Herberhold, H.; Royer, C. A.; Winter, R. *Biochemistry* **2004**, *43*, 3336.
(16) Kitchen, D. B.; Reed, L. H.; Levy, R. M. *Biochemistry* **1992**, *31*, 10 083.
(17) Paci, E. *Biochim. Biophys. Acta* **2002**, *1595*, 185.
(18) Kovalenko, A. Three-Dimensional RISM Theory for Molecular Liquids and Solid-Liquid Interfaces. In *Molecular Theory of Solvation*; Hirata, F., Ed.; Kluwer: Dordrecht, The Netherlands, 2003; pp 169−275.
(19) Beglov, D.; Roux, B. *J. Chem. Phys.* **1995**, *103*, 360.

(20) Kovalenko, A.; Hirata, F. *Chem. Phys. Lett.* **1998**, *290*, 237.
(21) Kovalenko, A.; Hirata, F. *J. Phys. Chem. B* **1999**, *110*, 10 095.
(22) Kovalenko, A. Hirata, F. *J. Chem. Phys.* **2000**, *112*, 10 391.
(23) Imai, T.; Kovalenko, A.; Hirata, F. *Chem. Phys. Lett.* **2004**, *395*, 1.
(24) Smith, P. E. *Biophys. Chem.* **2005**, *113*, 299.
(25) Damjanovíc, A.; García-Moreno, B.; Lattman, E. E.; García, A. E. *Proteins: Struct., Funct., Bioinf.* **2005**, *60*, 433.
(26) Humphrey, W.; Dalke, A.; Schulten, K. *J. Mol. Graphics* **1996**, *14*, 33.
(27) MacKerell, A. D., Jr.; Bashford, D.; Bellott, M.; Dunbrack, R. L., Jr.; Evanseck, J. D.; Field, M. J.; Fischer, S.; Gao, J.; Guo, H.; Ha, S.; Joseph-McCarthy, D.; Kuchnir, L.; Kuczera, K.; Lau, F. T. K.; Mattos, C.; Michnick, S.; Ngo, T.; Nguyen, D. T.; Prodhom, B.; Reiher, W. E., III; Roux, B.; Schlenkrich, M.; Smith, J. C.; Stote, R.; Straub, J.; Watanabe, M.; Wiorkiewicz-Kuczera, J.; Yin, D.; Karplus, M. *J. Phys. Chem. B* **1998**, *102*, 3586.
(28) Jorgensen, W. L.; Chandrasekhar, J.; Madura, J. D.; Impey, R. W.; Klein, M. L. *J. Chem. Phys.* **1983**, *79*, 926.
(29) Kalé, L.; Skeel, R.; Bhandarkar, M.; Brunner, R.; Gursoy, A.; Krawetz, N.; Phillips, J.; Shinozaki, A.; Varadarajan, K.; Schulten, K. *J. Comput. Phys.* **1999**, *151*, 283.
(30) Kirkwood, J. G.; Buff, F. P. *J. Phys. Chem.* **1951**, *19*, 774.
(31) Harano, Y.; Imai, T.; Kovalenko, A.; Kinoshita, M.; Hirata, F. *J. Phys. Chem.* **2001**, *114*, 9506.
(32) Duffy, E. M.; Severance, D. L.; Jorgensen, W. L. *Isr. J. Chem.* **1993**, *33*, 323.
(33) Jorgensen, W. L. *J. Phys. Chem.* **1986**, *90*, 1276.
(34) Callam, C. S.; Singer, S. J.; Lowary, T. L.; Hadad, C. M. *J. Am. Chem. Soc.* **2001**, *123*, 11 743.
(35) Bagchi, K.; Balasubramanian, S.; Klein, M. L. *J. Chem. Phys.* **1997**, *107*, 8561.
(36) Paliwal, A.; Asthagiri, D.; Bossev, D. P.; Paulaitis, M. E. *Biophys. J.* **2004**, *87*, 3479.
(37) Smolin, N.; Winter, R. *Biochim. Biophys. Acta* **2006**, *1764*, 522.
(38) Paschek, D.; García, A. E. *Phys. Rev. Lett.* **2004**, *93*, 238 105.
(39) Paschek, D.; Gnanakaran, S.; Garcia, A. E. *Proc. Natl. Acad. Sci. U.S.A.* **2005**, *102*, 6765.
(40) Gekko, K.; Timasheff, S. N. *Biochemistry* **1981**, *20*, 4667.
(41) Gekko, K.; Timasheff, S. N. *J. Biochem.* **1981**, *91*, 1197.
(42) Priev, A.; Almagor, A.; Yedgar, S.; Gavish, B. *Biochemistry* **1996**, *35*, 2061.
(43) Timasheff, S. N. *Biochemistry* **2002**, *41*, 13 473.
(44) Filfil, R.; Chalikian, T. V. *J. Mol. Biol.* **2000**, *299*, 827.
(45) Chalikian, T. V.; Breslauer, K. J. *Biopolymers* **1996**, *39*, 619.
(46) Terasawa, S.; Itsuki, H.; Arakawa, S. *J. Phys. Chem.* **1975**, *79*, 2345.
(47) Edward, J. T.; Farrell, P. G. *Can. J. Chem.* **1975**, *53*, 2965.
(48) Imai, T.; Harano, Y.; Kovalenko, A.; Hirata, F. *Biopolymers* **2001**, *59*, 512.
(49) Imai, T.; Kovalenko, A.; Hirata, F. *J. Phys. Chem. B* **2005**, *109*, 6658.